NISTIR 88-3817

Structural Reliability and Damage Tolerance of Ceramic Composites for High-Temperature Applications

Semi-Annual Progress Report for the Period Ending March 31, 1988

E. R. Fuller, Jr., T.W. Coyle, T.R. Palamides and R.F. Krause, Jr.

U.S. DEPARTMENT OF COMMERCE
National Institute of Standards and Technology
(Formerly National Bureau of Standards
Ceramics Division
Gaithersburg, MD 20899

August 1988

Interagency Agreement DE-AI05-800R206179

Prepared for
U.S. DEPARTMENT OF ENERGY
Fossil Energy
Advanced Research & Technology Development
Fossil Energy Materials Program
Oak Ridge National Laboratory
Oak Ridge, TN

NISTIR 88-3817

Structural Reliability and Damage Tolerance of Ceramic Composites for High-Temperature Applications

Semi-Annual Progress Report for the Period Ending March 31, 1988

E. R. Fuller, Jr., T.W. Coyle, T.R. Palamides and R.F. Krause, Jr.

U.S. DEPARTMENT OF COMMERCE
National Institute of Standards and Technology
(Formerly National Bureau of Standards
Ceramics Division
Gaithersburg, MD 20899

August 1988

Interagency Agreement DE-AI05-800R206179

National Bureau of Standards became the National Institute of Standards and Technology on August 23, 1988, when the Omnibus Trade and Competitiveness Act was signed. NIST retains all NBS functions. Its new programs will encourage improved use of technology by U.S. industry.

Prepared for
U.S. DEPARTMENT OF ENERGY
Fossil Energy
Advanced Research & Technology Development
Fossil Energy Materials Program
Oak Ridge National Laboratory
Oak Ridge, TN

U.S. DEPARTMENT OF COMMERCE
C. William Verity, Secretary

NATIONAL INSTITUTE OF STANDARDS AND TECHNOLOGY
Ernest Ambler, Director

STRUCTURAL RELIABILITY AND DAMAGE TOLERANCE OF CERAMIC COMPOSITES FOR HIGH-TEMPERATURE APPLICATIONS

Semi-Annual Progress Report for the Period Ending March 31, 1988 *

Prepared for US Department of Energy, Fossil Energy
Advanced Research & Technology Development
Fossil Energy Materials Program
Oak Ridge National Laboratory
Oak Ridge, TN

E. R. Fuller, Jr., T. W. Coyle,
T.R. Palamides and R. F. Krause, Jr.

National Bureau of Standards
Institute for Materials Science and Engineering
Ceramics Division
Gaithersburg, MD 20899

INTRODUCTION

The achievement of higher efficiency heat engines and heat recovery systems requires the availability of high-temperature, high-performance structural materials. Structural ceramics, and more recently, ceramic matrix composites have received particular attention for these applications due to their high strength, and resistance to corrosion and thermal shock. Even with these positive attributes, improved reliability and extended lifetime under service conditions are necessary for structural ceramics to gain industrial acceptance. The problems with these materials are mechanical and chemical in nature and are enhanced by the fact that they are subjected to high temperatures, reactive environments and extreme thermal gradients.

With an objective of improved performance for heat engine/heat recovery applications, the NBS program on structural ceramics and ceramic composites addresses these problems through the determination of critical factors that influence mechanical and microstructural behavior. The activities of the program are grouped under two major subtasks, each designed to develop key data, associated test methods and companion predictive models. The status of the subtasks are detailed in the following sections.

* Also in ORNL/FMP-88/1, Fossil Energy Materials Program, R.R. Judkins, Manager, Oak Ridge National Laboratory, Oak Ridge, TN, July 1988, pp. 103-116.

DISCUSSION OF CURRENT ACTIVITIES

Subtask A: Interfacial and Microstructural Composite Properties

Measurement of Fiber/Matrix Interfacial Forces

An indentation technique has been developed to characterize the mechanical behavior of the fiber/matrix interface in ceramic-ceramic composites under applied shear loads. A force is applied on the polished cross section of a specimen to a fiber parallel to the fiber axis. This results in a displacement of the fiber relative to the matrix surface. To determine the resistance to shear displacement along the fiber/matrix interface it is necessary to know the force applied to the fiber, the relative displacement between fiber and matrix, and the area of interface over which the displacement occurs. A Vickers hardness indenter instrumented to measure the load applied to the fiber and the displacement of the tip of the diamond indenter has been developed over the past year and is currently operational. The measured load-displacement curves can be used in conjunction with an appropriate mechanics analyses to characterize the behavior of the interface.

Preliminary measurements have been made on Nicalon fiber, glass ceramic (LAS III) composite to check out the system. These measurements are still in progress. Future studies will examine specimens of a Nicalon fiber-reinforced SiC composites provided by R.A. Lowden of Oak Ridge National Laboratory. These materials are 2-D reinforced composites produced at Oak Ridge National Laboratory by a chemical vapor infiltration (CVI) process. The goal of the testing is to relate the strength of the interface to the various interfacial structures produced during the CVI fabrication process.

Characterization of Matrix Crack - Fiber Interactions

Summary. The double cleavage drilled compression (DCDC) configuration has been used as a model composite system to study the influence of multiple fiber arrays and fiber coating on the toughening increment from fiber reinforcement. Heretofore, only cracks interacting with a single

fiber have been investigated. In this reporting period multiple linear arrays of fibers, up to three (3), have been investigated. In addition, studies have been initiated to examine the influence of fiber coating and coating thickness on the toughening increment. Metallic coatings of nickel from 1 μm to 22 μm have been examined. Results of these studies are reported below.

Multiple Fibers. The double cleavage drilled compression (DCDC) configuration has been used to study the influence of multiple fiber arrays on the toughening increment resulting from individual fibers. As previously reported [1,2], the specimen configuration is a DCDC specimen in the Janssen geometry [3]. Model composite systems have been simulated by the addition of individual SiC fibers (AVCO's SCS-6 fibers) in the borosilicate glass matrix.

The relationship between applied stress intensity factor and crack length for the DCDC specimens has been experimentally calibrated. Results agree reasonably well with previous analyses of this specimen [3-6]. There is still, however, an unexplained shift in the calibration curves, which result in an arbitrary shift in the resulting stress intensity factor curves. Although we are still working to determine the cause of this shift, its existence for the current experiments is unimportant, since we can normalize the original toughness to that of the glass matrix.

Specimens with one, two, and three fibers in a planar array along the crack front have been fabricated. Typical toughening increments for these cases are shown in Fig. 1. The one-fiber specimens had the fiber situated in the center of the specimen, which was 6.35 mm wide. The two-fiber array was arranged with the two fibers 3.18 mm apart and 1.59 mm from the edges. The three-fiber array was arranged with the fibers 1.59 mm apart and from the edges. As can be seen from Fig. 1, the two-fiber configuration resulted in a substantial toughening increment. However, the three-fiber configuration was less than what might be expected (i.e., less than the two-fiber array). This observation most likely resulted from the different processing conditions which were used for the two configurations. The 1.59 mm and the 3.18 mm glass slabs used to fabricate

these specimens, although nominally the same composition, appeared to have different surface conditions, which required different hot pressing conditions.

Fiber Coatings. In addition to the studies with multiple fiber arrays, studies have been initiated to examine the influence of fiber coating and coating thickness on the toughening increment. Nickel has been electrodeposited on the SiC fibers to a thickness of 1 μm to 22 μm. Typical results of these studies are shown in Fig. 2. Preliminary scanning electron microscopy has revealed microstructures which agree qualitatively with these results; namely, the 1 μm Ni coating appears to have made a strong bond with the glass matrix, whereas the thicker coating are not bonded as well.

Quantitative information regarding the closure forces exerted by bridging fiber requires knowledge of the interfacial shear resistance of the fiber-matrix interface. These interfacial properties can be evaluated by measuring the force required to push the fibers through thin sections of the glass matrix using the indentation technique discussed above. Such measurements will be included in further efforts to quantify the effects of the fibers on the toughening in these model composites.

Subtask B: High-Temperature Damage Modes and Failure Mechanisms

Creep and Creep Rupture Behavior

Summary. Creep and creep rupture behavior of a 25 wt percent silicon carbide whisker-reinforced alumina ceramic with 4.9 percent porosity was measured in four-point flexure at temperatures between 1100° and 1300°C. The applied stresses for these studies varied between 55 and 306 MPa. However, the applied stresses at each temperature varied over a much narrower range, typically by a factor of one and a half to two, with the high applied stresses at the low temperature, and vice versa. The composite materials were provided as billets through the courtesy of Dr. J. F. Rhodes of the Advanced Composite Materials Corporation [7]. Results of these experiments are reported below.

High-Temperature Flexural Strength. The flexural strength of this material was determined last reporting period as a function of temperature between 25 and 1300°C [2]. The strength remained approximately invariant at approximately 600 MPa to 900°C; beyond this temperature, it regressed to approximately half as strong at 1300°C.

Creep and Creep Rupture Behavior. The flexural creep specimens, 3 mm x 4 mm x 50 mm, were cut and ground the same as those used in the fracture toughness study [1,2,8] except they did not receive a finishing polish. They were mounted in place on silicon carbide platens with 6 mm diam loading rollers using nitrocellulose cement. A constant load was applied to the specimen through a pneumatic cylinder with a lubricated rubber diaphragm. A controlled-leak, pressure regulator was capable of maintaining the applied load within ± 2 N. The load was transmitted through 19 mm diam rods of 99 percent recrystallized silicon carbide, bearing on a hemi-spherical compression tool of the same material.

Three sets of loading rods protruded through the roof and floor of an alumina-insulated furnace cavity, 150 mm x 200 mm x 150 mm high, to accommodate two test specimens simultaneously. The third (central) loading rod was used as a reference leg to correct for strains resulting from expansion of the frame due to room temperature fluctuations. Four such furnace assemblies were used in these tests. All tests at a given temperature were conducted in the same furnace.

A pre-load of approximately 10 N maintained the specimen alignment, while heating to the test temperature, during which time the nitrocellulose cement burned away. The furnace cavity was heated to the test temperature in approximately one hour by molybdenum disilicide heating elements, radiating from the side walls within the furnace cavity. The temperature was controlled and measured by calibrated platinum-rhodium thermocouples. The loading rods were water-cooled where they were connected to air cylinders and load transducers, which were supported in the same frame above and below the furnace, respectively. The load transducers were calibrated with known weights. After the specimens reached the test temperature, the load was increased to a value corresponding to the pre-chosen applied stress, generally approximately half the material strength, or less.

The creep strain, ϵ, was characterized by measuring the loading-point displacement, y, as a function of time, t, and using the relation [9]:

$$\epsilon = 6\ yw/(\ell_1^2+\ell_1\ell_2-2\ell_2^2), \qquad (1)$$

where the specimen height is w = 3 mm, and the major and minor loading spans are ℓ_1 = 40 mm and ℓ_2 = 10 mm, respectively. The neutral axis of bending was assumed to be at the geometric center of the specimen and the stress exponent was assumed as unity. These assumptions provide a convenience by which the data can be analyzed.

The loading-point displacement during creep was monitored by a linear voltage displacement transducer that was attached to each water-cooled holder of an upper ram of the test equipment. The transducers were calibrated with known gauge blocks, and the displacement was measured within ± 5 μm. To enhance the long-term accuracy of the displacement readings, a block of silicon carbide, the same as that used for the rams, was used in the middle test station of a furnace. Any displacement measured on the block is believed to reflect changes in the test facility due mainly to fluctuations in the ambient temperature. These displacement fluctuations were substracted from the displacements measured on the specimens in the other two stations of the same furnace so that errors due to differential thermal expansion of the test facility were minimized. The failure of one specimen in a furnace was observed to have negligible effect on the other specimen, mainly because the pneumatic pistons and rubber shock absorbers were used to restrain the propagation of stress-waves.

Creep experiments on 32 specimens have been run to date, with some lasting up to sixteen hundred hours (1600 h). Table 1 gives a summary of the experiments conducted during this reporting period. Two regimes of behavior have been observed. See Figs. 3 and 4.

In the first regime, typified by the creep strain versus time curve in Fig. 3, only "primary" creep behavior is observed. Failure occurs in this regime with little or no evidence of steady-state or tertiary creep; the material "work-hardens" right up to the time of rupture. This apparent work-hardening characteristic of creep strain can be represented by

$$\epsilon = Ct^a, \qquad (2)$$

where a and C are constants. Least-squares fits of the logarithm of Eq. (2) show that the time exponent, a, appears to remain fairly constant over a range of applied stresses at a given temperature. See Figs. 5 through 7. This regime of response occurs for the larger applied stresses at a given temperature and for the higher temperatures at a given applied stress. In this failure regime the time-to-failure and the strain-to-failure increase with decreasing applied stress. This type of behavior has also been observed by Porter et al. [10] in the much higher temperature range around 1500° to 1600°C.

The second regime of behavior occurs for applied stresses below what appears to be an apparent threshold stress at each temperature. The creep behavior is typified by a large region of steady-state behavior; for example, see Fig. 4. The failure behavior is such that the strain at failure decreases with decreasing applied stress, although the time-to-failure is increasing; for example, see Fig. 7. The reasons for this behavior are not yet understood, but may be shown by in-progress microstructural examination of these specimens.

The threshold behavior between these two regimes becomes an important design consideration for this material. This is particularly exemplified at 1300°C, where a specimen at an applied stress of 72 MPa failed in less than 30 hours, while a specimen at 62 MPa has survived longer than 500 hours, thus far.

As a final comment, we noted a substantial degree of surface reactions on these specimens tested in air. Previously polished surfaces had their finishes dulled. Numerous pits were formed on the surface, which were on the order of 20 to 40 μm in diameter. The pits obscured microindents which were previously placed on the side of the creep specimen to monitor any shifts in the neutral strain axis during creep. Silica and mullite phases were also observed to form on surfaces under an applied stress, probably as a result of the oxidation of the SiC whiskers and a reaction with the alumina matrix.

REFERENCES

1. E.R. Fuller, Jr., T.W. Coyle, R.F. Krause, Jr., and T.J. Chuang, "Structural Reliability and Damage Tolerance of Ceramic Composites for High-Temperature Applications," Semiannual Progress Report ORNL/FMP-87/1, Fossil Energy Materials Program, R.R. Judkins, Manager, Oak Ridge National Laboratory, Oak Ridge, TN, July 1987, pp. 115-140.

2. E.R. Fuller, Jr., T.W. Coyle, and R.F. Krause, Jr., "Structural Reliability and Damage Tolerance of Ceramic Composites for High-Temperature Applications," Semiannual Progress Report ORNL/FMP-87/2, Fossil Energy Materials Program, R.R. Judkins, Manager, Oak Ridge National Laboratory, Oak Ridge, TN, February 1988, pp. 145-167.

3. C. Janssen, "Specimen for Fracture Mechanics Studies on Glass", Proceedings of the Xth International Congress on Glass, Kyoto, Japan, The Ceramic Society of Japan, 1974, pp. 23-30.

4. J.H. Henry, "Energie d'Avancement de Fissure, G, pour une Plaque Percee d'un Trou Soumise en Compression', Mechanics Research Communications 10 (5) 253-257 (1983).

5. C.G. Sammis and M.F. Ashby, "The Failure of Brittle Porous Solids Under Compressive Stress States", Act Metall. 34 511-526 (1986).

6. W.E. Warren, "Theoretical Analysis of the Double Cleavage Drilled Compression Specimen", Int. Journal of Fract. 33 223-325 (1987).

7. J.F. Rhodes, formerly ARCO Chemical Company, Greer, SC, May 14, 1986.

8. R.F. Krause, Jr. and E.R. Fuller, Jr., "Fracture Toughness Behavior of a Silicon Carbide Whisker-Reinforced Alumina Ceramic at Selected Porosities," in Fossil Energy Materials Program Conference Proceedings, ORNL/FMP-87/4, ed. by R.R. Judkins, Oak Ridge National Laboratory, Oak Ridge, TN, Aug. 1987, pp. 38-55.

9. G.W. Hollenberg, G.R. Terwilliger, and R.S. Gordon, "Calculation of Stresses and Strains in Four-Point Bending Creep Tests," J. Amer. Ceram. Soc. 54 196-199 (1971).

10. J. R. Porter and B. N. Cox, Bull. Am. Ceram. Soc. 67, 568 (1988).

Table 1. Creep rupture behavior of a 25 wt percent silicon carbide whisker-reinforced alumina ceramic having 4.9 wt percent porosity. Failure times and strains with a greater-than-symbol refer to specimens that have not yet ruptured up to the time and strain indicated.

Temperature °C	Stress σ (MPa)	Failure Time (hours)	Failure Strain (percent)
1100	231	139	0.175
	306	25.1	0.167
1145	175	262.4	0.621
	200	64.1	0.388
	224	35.6	0.390
	248	24.9	0.339
1200	123	>504	>0.75
	132	52	0.681
	147	60.8	1.178
	174	19.9	0.825
	174	27.2	0.872
	198	12.3	0.703
1245	82	>504	>0.35
	98	161.7	1.135
	122	27.0	1.858
	147	7.5	1.169
1300	55	>504	>0.247
	62	>504	>0.955
	72	27.6	1.846
	98	5.1	1.956

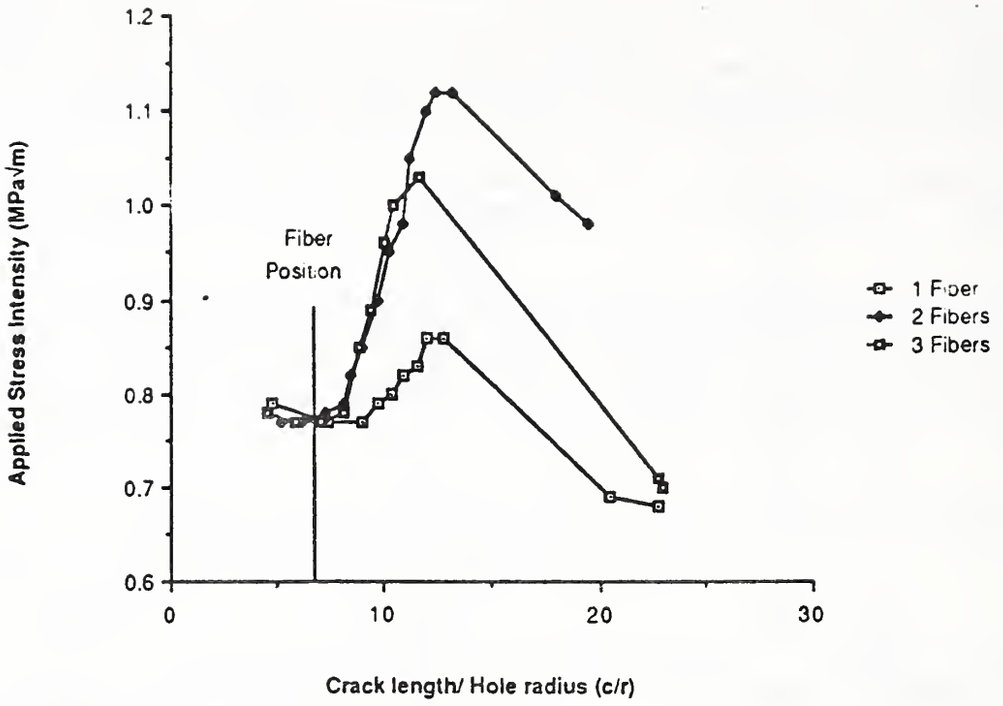

Figure 1. The toughening increment for double-cleavage drilled-compression (DCDC) specimens with one, two, and three planar arrays of fibers at the indicated position. The reduced toughening increment of the three fiber configuration, from what might be expected, most likely resulted from different processing conditions.

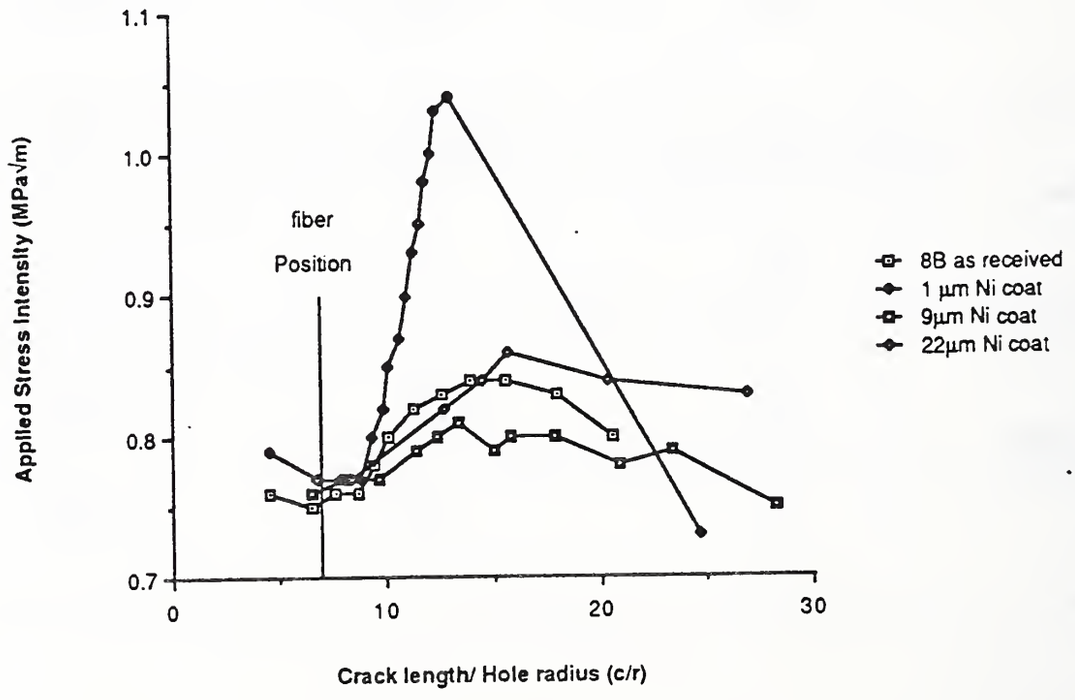

Figure 2. The toughening increment for double-cleavage drilled-compression (DCDC) specimens with a single nickel-coated fiber with various coating thicknesses.

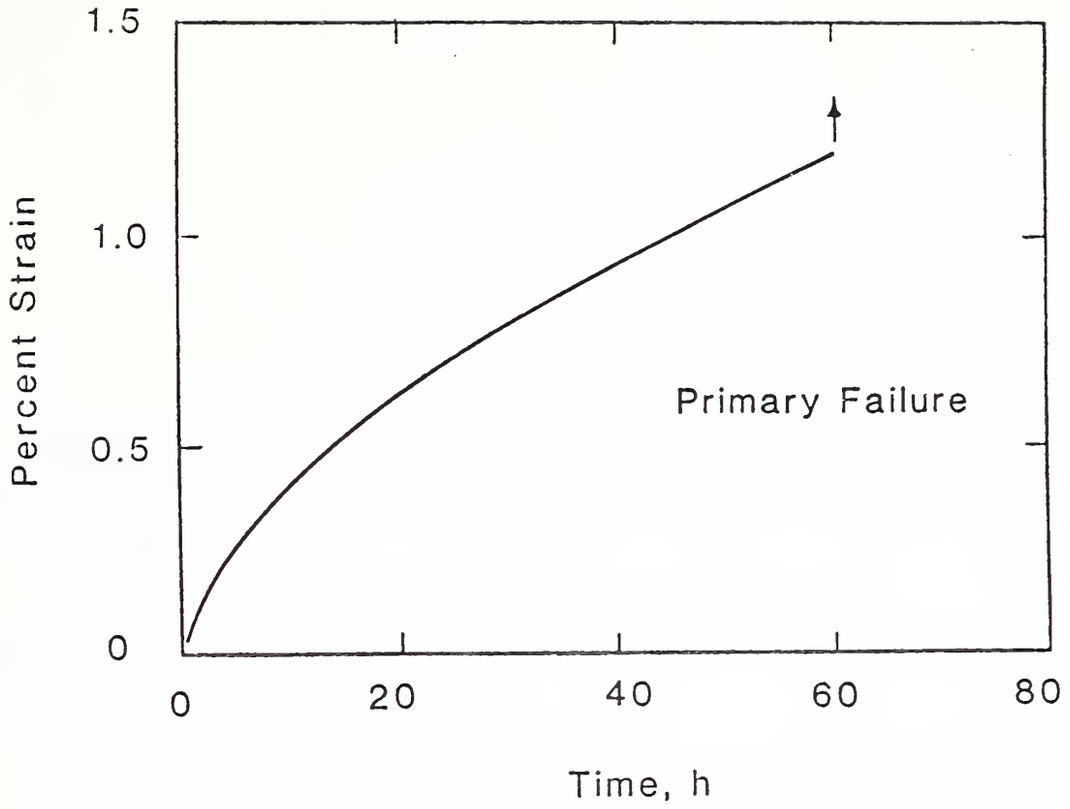

Figure 3. Typical creep curve of creep strain versus time in the "primary" creep regime. The data are for a flexure specimen of a 25 wt percent silicon carbide whisker-reinforced alumina ceramic of 4.9 percent porosity under the given applied stress of 147 MPa at 1200°C.

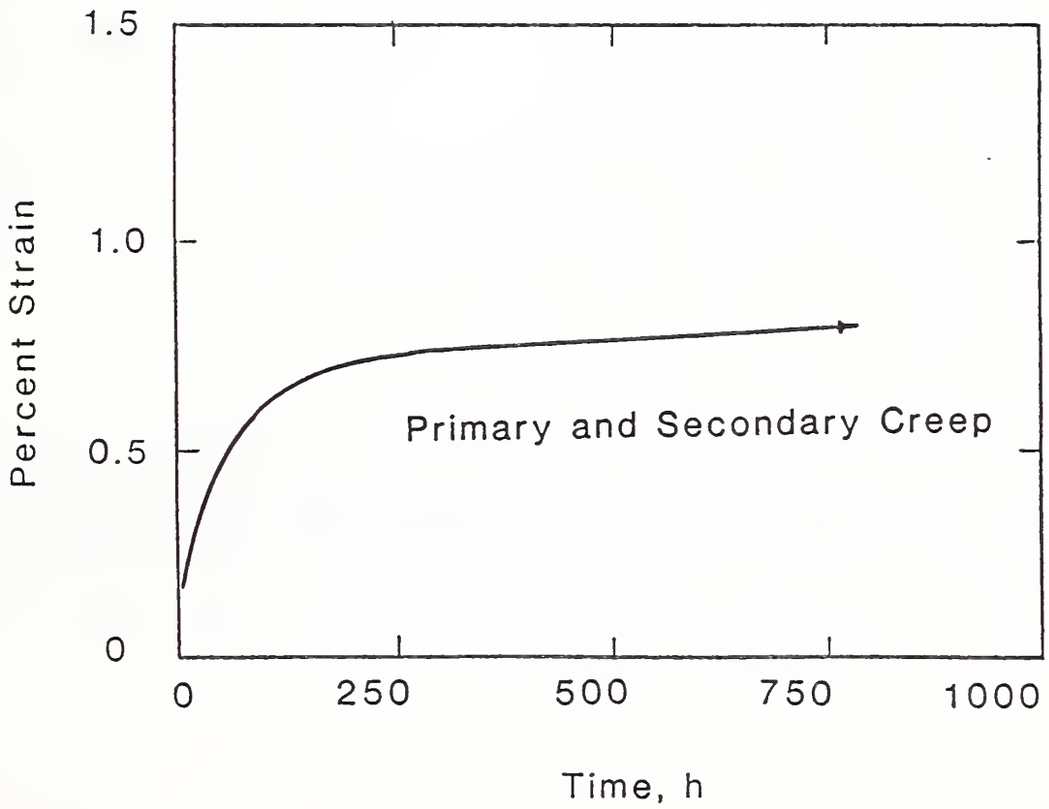

Figure 4. Typical creep curve of creep strain versus time in the "steady-state" creep regime. The data are for a flexure specimen of a 25 wt percent silicon carbide whisker-reinforced alumina ceramic of 4.9 percent porosity under the given applied stress of 123 MPa at 1200°C.

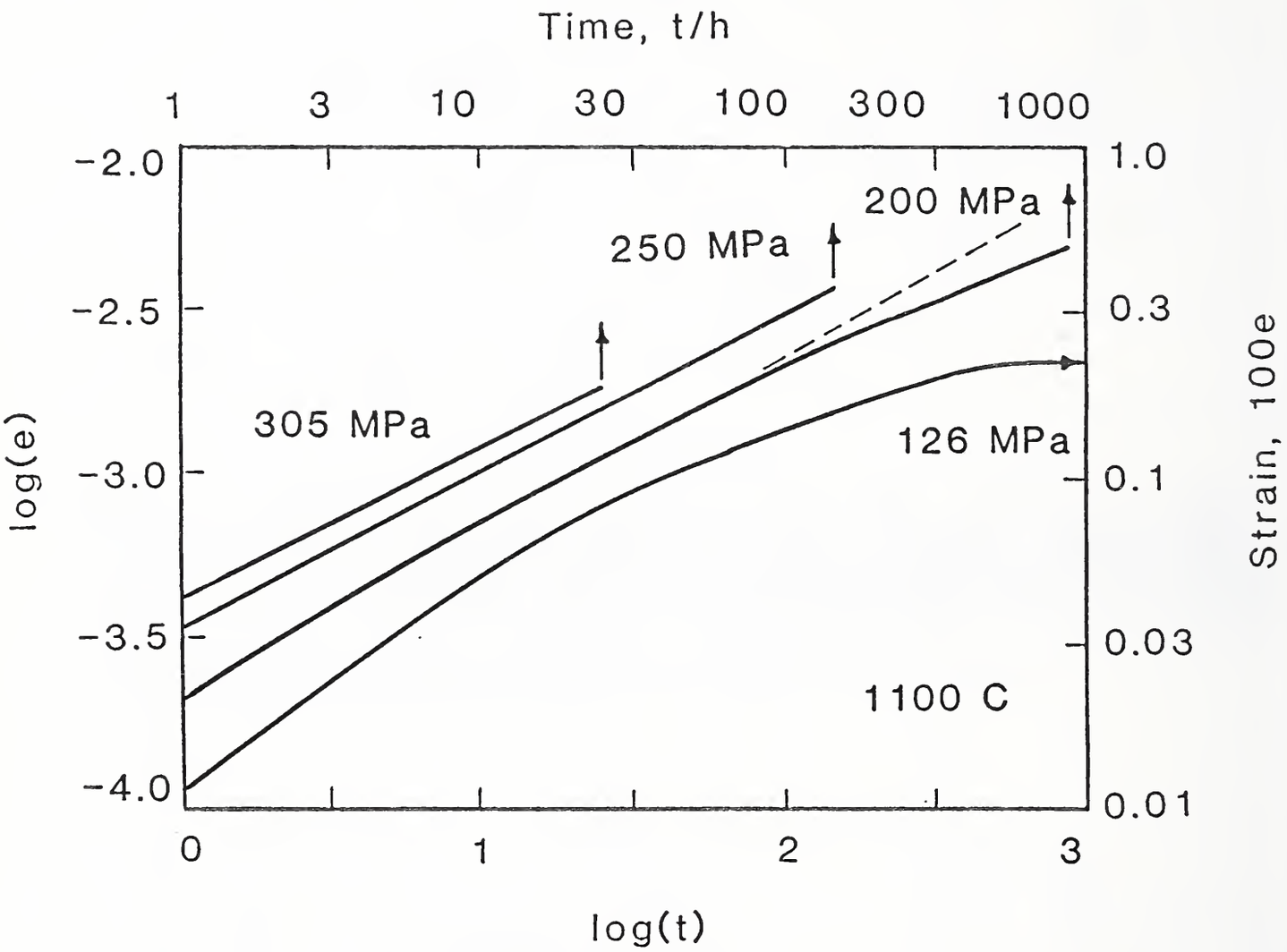

Figure 5. Logarithmic creep data at 1100°C (logarithm of creep strain versus logarithm of time) for flexural specimens of a 25 wt percent silicon carbide whisker-reinforced alumina ceramic of 4.9 percent porosity. Note the transition in behavior between applied stresses of 200 and 126 MPa.

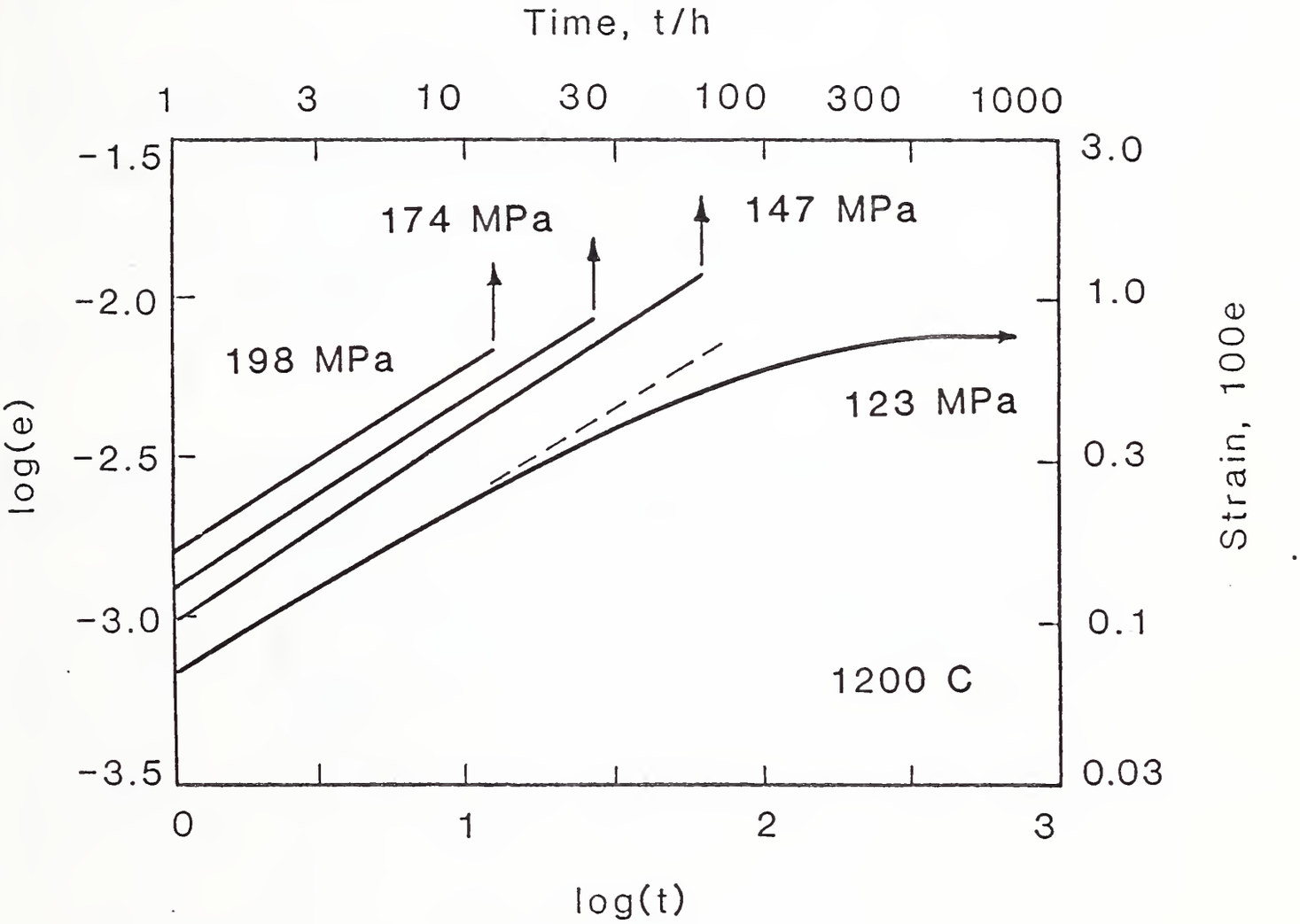

Figure 6. Logarithmic creep data at 1200°C (logarithm of creep strain versus logarithm of time) for flexural specimens of a 25 wt percent silicon carbide whisker-reinforced alumina ceramic of 4.9 percent porosity. Note the transition in behavior between applied stresses of 147 and 123 MPa.

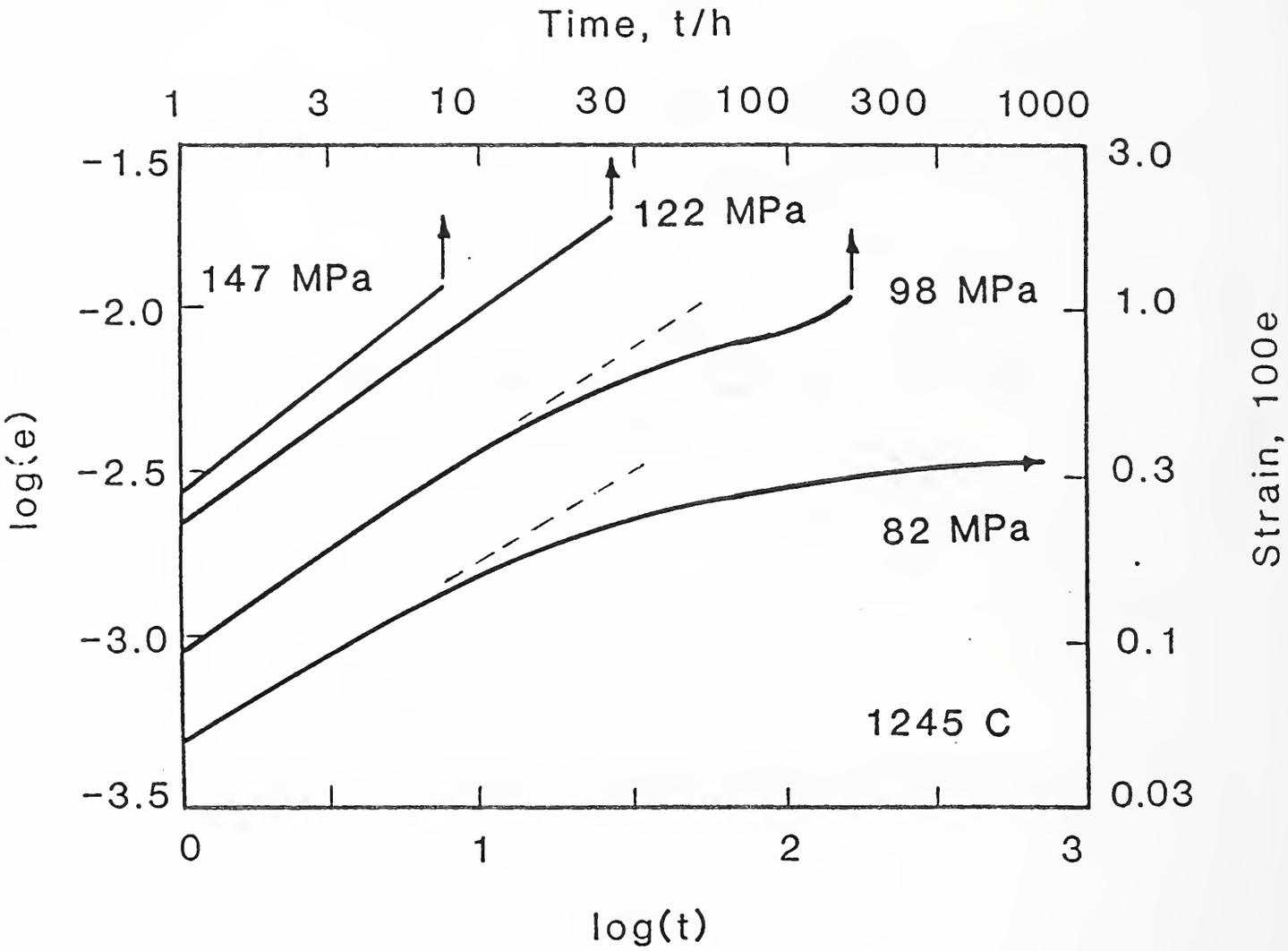

Figure 7. Logarithmic creep data at 1245°C (logarithm of creep strain versus logarithm of time) for flexural specimens of a 25 wt percent silicon carbide whisker-reinforced alumina ceramic of 4.9 percent porosity. Note the transition in behavior between applied stresses of 122 and 98 MPa.

NBS-114A (REV. 2-8C)

U.S. DEPT. OF COMM. BIBLIOGRAPHIC DATA SHEET (See instructions)	2. PUBLICATION OR REPORT NO. NISTIR 88-3817	3. Performing Organ. Report No.	3. Publication Date August 1988

4. TITLE AND SUBTITLE

Structural Reliability and Damage Tolerance of Ceramic Composites for High-Temperature Applications Semi-Annual Progress Report for the Period Ending March 31, 1988.

5. AUTHOR(S)

E.R. Fuller,Jr., T.W. Coyle, T.R. Palamides and R.F. Krause, Jr.

6. PERFORMING ORGANIZATION (If joint or other than NBS, see instructions)

NATIONAL BUREAU OF STANDARDS
U.S. DEPARTMENT OF COMMERCE
GAITHERSBURG, MD 20899

7. Contract/Grant No.

8. Type of Report & Period Covered

9. SPONSORING ORGANIZATION NAME AND COMPLETE ADDRESS (Street, City, State, ZIP)

U.S. Department of Energy
Fossil Energy, Advanced Research & Technology Development
Fossil Energy Material Program, Oak Ridge National Laboratory, Oak Ridge, TN

10. SUPPLEMENTARY NOTES

__ Document describes a computer program; SF-185, FIPS Software Summary, is attached.

11. ABSTRACT (A 200-word or less factual summary of most significant information. If document includes a significant bibliography or literature survey, mention it here)

The achievement of higher efficiency heat engines and heat recovery systems requires the availability of high-temperature, high-performance structural materials. Structural ceramics, and more recently, ceramic matrix composites have received particular attention for these applications due to their high strength, and resistance to corrosion and thermal shock. Even with these positive attributes, improved reliability and extended lifetime under service conditions are necessary for structural ceramics to gain industrial acceptance. The problems with these materials are mechanical and chemical in nature and are enhanced by the fact that they are subjected to high temperatures, reactive environments and extreme thermal gradients.

With an objective of improved performance for heat engine/heat recovery applications, the NBS program on structural ceramics and ceramic composites addresses these problems through the determination of critical factors that influence mechanical and microstructural behavior. The activities of the program are grouped under two major subtasks, each designed to develop key data, associated test methods and companion predictive models. The status of the subtasks are detailed in the following sections.

12. KEY WORDS (Six to twelve entries; alphabetical order; capitalize only proper names; and separate key words by semicolons)

Composites; double-cleavage-drilled-compression; indentation; R-curve; SiC fibers; SiC Whiskers; shear resistance; strength

13. AVAILABILITY

X Unlimited

__ For Official Distribution. Do Not Release to NTIS

__ Order From Superintendent of Documents, U.S. Government Printing Office, Washington, D.C. 20402.

X Order From National Technical Information Service (NTIS), Springfield, VA. 22161

14. NO. OF PRINTED PAGES

17

15. Price

$9.95

USCOMM-DC 6043-P80